Mode-specific reactivity of CH_4 on Pt(110)-(1×2): The concerted role of stretch and bend excitation

Régis Bisson,[*] Marco Sacchi,[†] and Rainer D. Beck

Laboratoire Chimie Physique Moléculaire, Ecole Polytechnique Fédérale de Lausanne, CH-1015 Lausanne, Switzerland

(Received 9 August 2010; published 9 September 2010)

The state-resolved reaction probability of CH_4 on Pt(110)-(1×2) was measured as a function of CH_4 translational energy for four vibrational eigenstates comprising different amounts of C-H stretch and bend excitation. Mode-specific reactivity is observed both between states from different polyads and between isoenergetic states belonging to the same polyad of CH_4. For the stretch/bend combination states, the vibrational efficacy of reaction activation is observed to be higher than for either pure C-H stretching or pure bending states, demonstrating a concerted role of stretch and bend excitation in C-H bond scission. This concerted role, reflected by the nonadditivity of the vibrational efficacies, is consistent with transition state structures found by *ab initio* calculations and indicates that current dynamical models of CH_4 chemisorption neglect an important degree of freedom by including only C-H stretching motion.

Methane (CH_4) dissociation on transition-metal surfaces is of great interest in the context of hydrogen production since it is the rate limiting step in the steam reforming process, the principal route for the transformation of CH_4 into H_2. Despite the 15 molecular degrees of freedom associated with the CH_4/surface system, the elementary step in the dissociative chemisorption of CH_4 consists of breaking a single C-H bond[1] and C-H stretch excitation has been shown to activate CH_4 dissociation on transition-metal surfaces.[2,3] We previously reported that the efficacy of the antisymmetric C-H stretch overtone state ($2\nu_3$) for promoting CH_4 dissociation is higher on Ni(111) than on Pt(111) and proposed that this difference in activation is related to the transition state structure with a larger bond length for the dissociating C-H bond on the Ni(111) surface.[4] A *ab initio* calculations performed by Nave and Jackson[5] are in agreement with this interpretation. These results imply a significant participation of C-H bond stretch in the reaction coordinate and might indicate that reduced dimensionality models including only C-H stretch motion can describe the essential feature of the reaction dynamics. Nevertheless other degrees of freedom may also contribute to the reaction coordinate. A survey of first-principles calculations of transition states for CH_4/metal systems[6–8] shows transition state structures of CH_4 with the dissociating C-H bond not only stretched but also bent from the equilibrium tetrahedral angle. Therefore, a realistic reaction coordinate might be expected to contain both C-H stretch and bend excitation. However, all dynamical models of methane dissociation published to date treat CH_4 as a "pseudodiatomic" containing a H_3C-H bond that can only be stretched.[5,9–11] State-resolved measurement by Juurlink *et al.*[12] find the $3\nu_4$ bend overtone to have a lower efficacy than the ν_3 stretch fundamental in activating CH_4 dissociation on nickel surfaces lending support to the reduced dimensionality assumption of these dynamical models but the complete neglect of bending motion is almost certainly an oversimplification.

In this Rapid Communication, we present a state-resolved study of CH_4 dissociative chemisorption on Pt(110)-(1×2) which measures the reaction probability of CH_4 prepared in four different vibrational eigenstates comprising different amounts of stretch and bend excitation. We observed that three nearly isoenergetic vibrational states each lead to significantly different dissociation probabilities whereas two states with different vibrational energy results in very similar reactivity. These observations provide clear evidence for mode-specific reactivity for CH_4 on Pt(110)-(1×2) which contradicts a basic assumption of statistical reaction rate theory.[13] Furthermore, the different efficacies for promoting the reaction of these four vibrational states provide information on the relevant degrees of freedom that theoretical models should consider to give a realistic description of CH_4 dissociation dynamics.

State-resolved reaction probability measurements are performed in an apparatus that consists of a molecular-beam source connected to an ultrahigh-vacuum chamber (base pressure 6×10^{-11} mbar).[14] We generate a pulsed molecular beam of CH_4 with variable translation energy (E_t) by expanding different mixtures of CH_4 in H_2, He, or Ar carrier gas using nozzle temperatures of 323–373 K. The E_t of CH_4 is determined by time-of-flight measurements using a chopper wheel and an on-axis quadrupole mass spectrometer (QMS). Before CH_4 collides with the Pt(110)-(1×2) surface, we excite a significant fraction of the CH_4 molecules to a stationary molecular eigenstate[15] by pulsed infrared (IR) laser radiation with narrow bandwidth (0.02 cm^{-1}) and high energy (140 mJ/pulse). The tunable IR radiation is focused by a cylindrical lens to excite a 20 mm slice of the molecular beam 25 mm from the target surface. We use cavity ring-down spectroscopy in a separate free-jet expansion to tune the excitation laser into resonance with the selected rovibrational transition, to monitor that the resonance is maintained during the deposition time, and to determine the rotational level population of CH_4 in the jet expansion needed to determine the fraction of excited molecules. The laser fluence is sufficient to completely saturate the first overtone transition of the IR-active C-H stretch (~ 6000 cm^{-1}) and the stretch/bend combinations and bend overtone (~ 4300 cm^{-1}) of CH_4, which is verified experimentally by recording the laser fluence dependence of the laser-on depo-

TABLE I. CH_4 vibrational eigenstates excited in this study and their zero-order normal-mode label, vibrational energy E_{vib} (kJ/mol), fitted shift along the E_t axis $\Delta E_t^{\nu_i}$ (kJ/mol), and calculated vibrational efficacy η_{ν_i} (%).

Zero-order label	E_{vib}	$\Delta E_t^{\nu_i}$	η_{ν_i}
$\nu_1 + \nu_4$ (stretch/bend)	50.6	33.9 ± 1.1	66.9 ± 2.1
$\nu_3 + \nu_4$ (stretch/bend)	51.8	28.1 ± 1.2	54.3 ± 2.3
$2\nu_3$ (pure stretch)	72.1	33.6 ± 1.3	46.6 ± 1.8
$2\nu_2 + \nu_4$ (pure bend)	52.2	20.9 ± 1.3	40.2 ± 2.6

sition signal. The Pt(110) surface is cleaned by Ar^+ sputtering/annealing cycles until impurities can no longer be detected by Auger electron spectroscopy (AES). To determine absolute reaction probabilities for CH_4, we perform a timed exposure of the clean crystal surface to the molecular beam, measuring both the incident dose of CH_4 molecules per unit area with the calibrated QMS as well as the resulting coverage of carbon reaction products on the surface by performing calibrated AES measurements across the surface in a computer-controlled scan.[16]

We measured the state-resolved reactivity of CH_4, prepared in the four different vibrational states shown in Table I; each containing different amounts of C-H stretch and bend excitation given approximately by their zero-order normal-mode labels (ν_1 and ν_3 are the symmetric and antisymmetric stretch modes and ν_2 and ν_4 are IR-inactive and IR-active bend vibrations, respectively). Because of the near degeneracy of the stretch fundamentals and bend overtones, the vibrational states of CH_4 can be grouped into polyads of nearly isoenergetic vibrational states[17] (Fig. 1). The states $2\nu_2 + \nu_4$, $\nu_1 + \nu_4$, and $\nu_3 + \nu_4$ states are members of the octad, whereas $2\nu_3$ is part of the tetradecad. The zero-order normal-mode labels $2\nu_2 + \nu_4$, $\nu_1 + \nu_4$, and $\nu_3 + \nu_4$ are good descriptors of the octad states,[18] while the state labeled $2\nu_3$ contains about 15% $\nu_1 + \nu_3$ character both of which are pure stretching modes. Therefore, we consider the four eigenstates prepared in this study as pure bend ($2\nu_2 + \nu_4$), stretch/bend combinations ($\nu_1 + \nu_4$, $\nu_3 + \nu_4$) and pure stretch states ($2\nu_3$).

Figure 1 shows the result of an AES analysis of carbon product coverage across the Pt(110)-(1×2) surface after two subsequent CH_4 molecular-beam exposures (E_t =22.4 kJ/mol) in different positions on the surface. For

FIG. 1. (Color online) Dissociation product density on Pt(110)-(1×2) after two exposures to CH_4 beams excited in different isoenergetic vibrational eigenstates belonging to the octad.

each deposition, a different vibrational eigenstate of CH_4 was excited by tuning the laser to the corresponding R(1) rovibrational transition. The laser fluence was sufficient to completely saturate the excitation producing identical fractions of state-prepared CH_4 because the excitation used the same initial state ($v=0$, $J=1$) in either case. The two eigenstates, $2\nu_2 + \nu_4$ and $\nu_1 + \nu_4$, have very similar vibrational energy (Table I) but lead to different reactivity as seen in Fig. 1. $\nu_1 + \nu_4$ excitation of CH_4 in the incident molecular beam produced a 50% higher carbon product coverage even though the incident dose was only half of what was used in the $2\nu_2 + \nu_4$ deposition. This and similar data where two (or more) nearly isoenergetic states result in different reaction probabilities provide clear evidence of mode-specific reactivity of CH_4 on Pt(110)-(1×2). For mode-specific reactivity, the reaction probability is not only a function of the total available energy but depends on the specific eigenstate of the reagent molecule. Mode-specific reactivity of CH_4 has been observed previously on Ni(100) for the C-H stretch fundamentals (ν_1 and ν_3) (Refs. 2 and 19) and for both Ni(100) and Ni(111) comparing the bend overtone $3\nu_4$ with the C-H stretch fundamental ν_3.[12] The observation of mode specificity in CH_4 dissociation demonstrates the failure of the statistical rate theory[13] to capture the microscopic dynamics of CH_4 chemisorption on nickel and platinum surfaces.

Mode-specific reactivity for states of the octad provides information regarding intramolecular vibrational redistribution (IVR) during the methane/metal collision. We note that the narrow band excitation laser prepares a stationary rovibrational eigenstate of the isolated CH_4 in each case, which does not undergo IVR during the 10–20 μs flight time toward the target surface. However, close to the surface IVR becomes possible when the incident CH_4 starts to interact with the metal surface. The initially prepared eigenstate of the isolated molecule is not an eigenstate of the combined molecule/surface system and therefore can undergo a time evolution as the molecule approaches the surface which is referred to as "surface-induced IVR." Mode specificity will only be observable if surface-induced IVR is incomplete on the time scale of the molecule/surface interaction which is less than a picosecond for the range of incident speeds used here (690–2835 m/s). Halonen *et al.* have modeled this surface-induced IVR process within a reduced-dimensionality vibrationally adiabatic framework comprising the C-H stretch states including their first overtones. The eigenenergies of the CH_4/metal system were calculated as a function of the molecule/surface distance.[20] The resulting adiabatic vibrational energy curves and associated wave functions predict different vibrational energy flow and localization for different initial states. Halonen *et al.* suggested that mode specificity in the reaction is due to at least partially adiabatic motion along these vibrational energy curves. Nonadiabatic effects can occur near avoided curve crossings and because the number of avoided crossings increases for higher polyads, surface-induced IVR can be expected to accelerate with increasing vibrational energy. One might also expect intrapolyad surface-induced IVR to be faster than IVR between states belonging to different polyads due to smaller energy gaps. Therefore, surface-induced IVR may reduce or suppress mode specificity for states of higher poly-
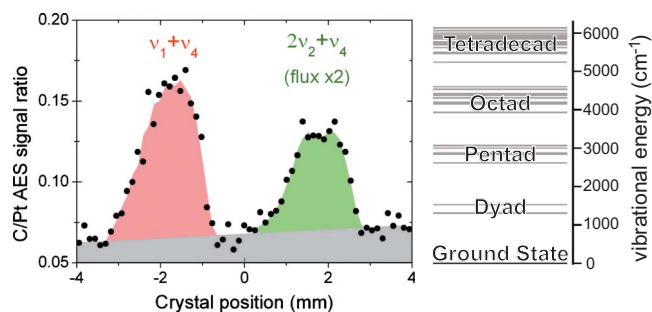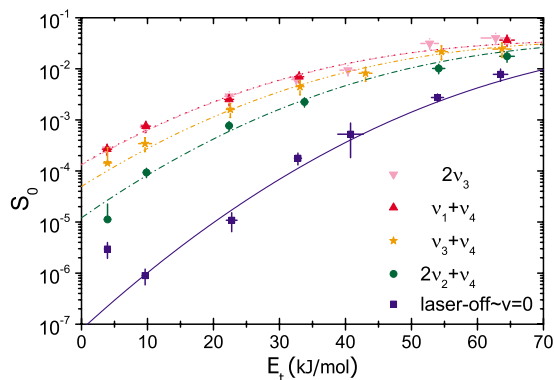
FIG. 2. (Color online) CH$_4$ state-resolved reactivity as a function of translational energy (E_t). $\nu_3+\nu_4$ and $2\nu_2+\nu_4$ reactivities at $E_t=4$ kJ/mol are upper limits. The error bars represent 95% confidence interval of the convoluted uncertainties. Lines are S-shaped reactivity curves fitted to data points.

ads and/or when comparing different vibrational states belonging to the same polyad. In past experiments, mode-specific reactivity within the same polyad has only been observed at the level of the C-H stretch fundamentals ν_1 and ν_3 (Refs. 2 and 19) which belong to the pentad, a group of five vibrational levels. Here, we observed mode-specific reactivity for states belonging to the octad, a higher polyad grouping eight vibrational levels. This shows that surface-induced IVR is far from complete for eigenstates belonging to the octad which raises the limit of vibrational energy at which mode-specific reactivity has been observed for CH$_4$ dissociation on a metal surface. IVR rates may be studied theoretically using recent high-dimensionality models which explicitly treat nonadiabatic couplings arising from the molecule/surface interaction,[21] if extended to combination and overtone eigenstates.

Figure 2 shows the state-resolved reactivity (S_0) of the CH$_4$ ground state ($v=0$) and four CH$_4$ vibrationally excited eigenstates on Pt(110)-(1×2) as a function of CH$_4$ translational energy (E_t). The nearly exponential increase in reactivity with E_t for $E_t>10$ kJ/mol is typical of a direct chemisorption mechanism, i.e., a single collision process. The state-resolved reactivity for $E_t<10$ kJ/mol has been discussed elsewhere.[16] While the $2\nu_2+\nu_4$, $\nu_1+\nu_4$, and $\nu_3+\nu_4$ states have similar vibrational energy (Table I), they result in different reactivities. Furthermore, the $\nu_1+\nu_4$ and $2\nu_3$ states have similar reactivities even though their vibrational energy is different. Mode-specific reactivity of CH$_4$ on Pt(110)-(1×2) is observed for each of the different vibrational eigenstates over a wide range of E_t. In order to compare more quantitatively the state-resolved activation of CH$_4$ dissociation on Pt(110)-(1×2), we use so-called S-shaped reactivity curves to parametrize our state-resolved data by least square fitting. The analytical form of the reactivity curves was initially proposed by Luntz,[22]

$$S_0[E_t] = \frac{A}{2}\left[1 + \text{erf}\left(\frac{E_t - E_0}{W}\right)\right], \qquad (1)$$

where A is the asymptotic value of S_0 at high E_t, W is the width of a Gaussian distribution of barrier heights defining

the slope of the S-shaped curve, and E_0 is the average barrier height where for $E_t=E_0$, S_0 reaches half of its asymptotic value A. Similar curve fitting was used by Utz and co-workers for Ni surfaces[23] and by our group for Pt surfaces[16] to parametrize state-resolved CH$_4$ reactivity data obtained over a wide range of E_t by the three fitting parameters. Free optimization of A, W, and E_0 leads to similar A and W values but different values of E_0. We therefore fix A and W to their average values, $A=0.037$ and $W=25$ kJ/mol, and optimize E_0 for the five sets of state-resolved data resulting in four congruent reactivity curves that can be superimposed with the $v=0$ reactivity curve by different shifts along the E_t axis. For a given state ν_i, the ratio of the shift $\Delta E_t^{\nu_i}=E_0(v=0) -E_0(\nu_i)$ to the corresponding vibrational energy $h\nu_i$ defines the vibrational efficacy η_{ν_i},[23,24]

$$\eta_{\nu_i} = \frac{\Delta E_t^{\nu_i}}{h\nu_i}. \qquad (2)$$

A summary of $\Delta E_t^{\nu_i}$ values and calculated vibrational efficacies can be found in Table I. $\eta_{\nu_i}<1$ indicates that it takes less than the equivalent to $h\nu_i$ in E_t to raise the reactivity of CH$_4$($v=0$) by the same amount as observed for excitation of the state ν_i, therefore CH$_4$ translation is more effective than the investigated CH$_4$ vibrations to increase the reaction rate on Pt(110)-(1×2). Furthermore, it can be seen that the two stretch/bend combination eigenstates have the highest vibrational efficacies, followed by the pure stretch overtone and the pure bend overtone.

The fact that the highest vibrational efficacies are observed for the stretch/bend combination states is striking. So far it was commonly assumed that stretch excitation is far more important in activating CH$_4$ dissociation than bend excitation[20,25] leading to reduced-dimensionality models which include only C-H stretch coordinates.[9–11] In contrast to this assumption, the present results demonstrate that concerted stretch and bend excitation results in a larger efficacy than either pure stretch or pure bend excitation. This concerted role of stretch and bend excitation is reflected by the observation that the vibrational efficacies of the stretch/bend combination states cannot simply be predicted as energy weighted averages of the efficacies of the contributing normal modes, i.e., the efficacies are apparently nonadditive.

The observed mode specificity, expressed by the ordering of the vibrational efficacies, is consistent with transition state structure calculations for CH$_4$ dissociation on the Pt(110)-(1×2) surface[6,8] which shows that the dissociating C-H bond is not only stretched but also bent. Our results underline the important role of *ab initio* calculations in defining the reaction coordinate for CH$_4$ dissociative chemisorption on metal surfaces. We suggest that dynamical calculations should consider not only the C-H stretch but include at least the bending angle between the dissociating C-H bond and the C$_3$ axis of the spectator methyl in order to more realistically describe the dynamics of CH$_4$ chemisorption.

We note that, similar to what was observed on Ni(100) and Ni(111),[12] the pure bending state of CH$_4$ has a lower efficacy than the pure stretching state on Pt(110)-(1×2).

Previously, Juurlink *et al.*[12] suggested that this sort of difference in efficacy might be due to different coupling of stretch vs bend quanta to low-frequency surface phonons. The fact that we observe a higher efficacy for the stretch/bend combination state $\nu_3 + \nu_4$ than for the $2\nu_3$ state, contradicts this suggestion. Finally, it is interesting that the stretch/bend combination state $\nu_1 + \nu_4$ shows a higher efficacy than the stretch/bend combination state $\nu_3 + \nu_4$. This is reminiscent of the observation of a higher vibrational efficacy for the ν_1 state compared to the ν_3 state of CH_4 on Ni(100) (Ref. 19) but further theoretical studies will be needed to understand if the observed mode specificity for these two pairs of states shares a common origin.

In conclusion, the measured state-resolved reactivity of CH_4 on Pt(110)-(1×2) for four vibrational eigenstates with different combinations of stretching and bending motion enable a detailed comparison of the role of stretch and bend excitation of CH_4 in its dissociative chemisorption. Vibrationally mode-specific reactivity is observed both between eigenstates belonging to different polyads and between states belonging to the same polyad which confirms that surface-induced IVR is inefficient and incomplete on the time scale of the reactive methane/metal encounter. These results contradict the fundamental assumption of statistical theories for calculating the reaction rate, invalidating them from a realistic description of the chemisorption dynamics of CH_4 on Pt(110)-(1×2). Vibrational efficacies are found to be higher for the two stretch/bend combination states than for the pure stretching and pure bending states, demonstrating their nonadditivity. The observation of a concerted role of stretching and bending motion in activating CH_4 dissociative chemisorption calls for the inclusion of both stretching and bending degrees of freedom in dynamical models, in contrast to previously reported reduced-dimensionality models that include only stretch excitations. Finally, mode-specific chemisorption of CH_4 is not unique to Ni surfaces and follows similar trends on Pt(110)-(1×2). Dynamical calculations performed on a realistic multidimensional potential-energy surface of this benchmark gas-surface system are needed to understand these trends, not only for CH_4 fundamental vibrational modes but also for CH_4 combination and overtone states.

*regis.bisson@polytechnique.edu

†Present Address: Surface Science Group, Department of Chemistry, University Of Cambridge, Lensfield Road, Cambridge CB2 1EW, United Kingdom.

[1] M. B. Lee, Q. Y. Yang, S. L. Tang, and S. T. Ceyer, J. Chem. Phys. **85**, 1693 (1986).

[2] L. B. F. Juurlink, P. R. McCabe, R. R. Smith, C. L. DiCologero, and A. L. Utz, Phys. Rev. Lett. **83**, 868 (1999).

[3] J. Higgins, A. Conjusteau, G. Scoles, and S. L. Bernasek, J. Chem. Phys. **114**, 5277 (2001).

[4] R. Bisson, M. Sacchi, T. T. Dang, B. Yoder, P. Maroni, and R. D. Beck, J. Phys. Chem. A **111**, 12679 (2007).

[5] S. Nave and B. Jackson, J. Chem. Phys. **130**, 054701 (2009).

[6] A. T. Anghel, D. J. Wales, S. J. Jenkins, and D. A. King, Phys. Rev. B **71**, 113410 (2005).

[7] G. Henkelman, A. Arnaldsson, and H. Jonsson, J. Chem. Phys. **124**, 044706 (2006).

[8] S. Nave, A. K. Tiwari, and B. Jackson, J. Chem. Phys. **132**, 054705 (2010).

[9] A. P. J. Jansen and H. Burghgraef, Surf. Sci. **344**, 149 (1995).

[10] A. K. Tiwari, S. Nave, and B. Jackson, Phys. Rev. Lett. **103**, 253201 (2009).

[11] J. Harris, J. Simon, A. C. Luntz, C. B. Mullins, and C. T. Rettner, Phys. Rev. Lett. **67**, 652 (1991).

[12] L. B. F. Juurlink, R. R. Smith, D. R. Killelea, and A. L. Utz, Phys. Rev. Lett. **94**, 208303 (2005).

[13] H. L. Abbott, A. Bukoski, and I. Harrison, J. Chem. Phys. **121**, 3792 (2004).

[14] M. P. Schmid, P. Maroni, R. D. Beck, and T. R. Rizzo, Rev. Sci. Instrum. **74**, 4110 (2003).

[15] D. J. Nesbitt and R. W. Field, J. Phys. Chem. **100**, 12735 (1996).

[16] R. Bisson, M. Sacchi, and R. D. Beck, J. Chem. Phys. **132**, 094702 (2010).

[17] S. Albert, S. Bauerecker, V. Boudon, L. R. Brown, J.-P. Champion, M. Loëte, A. Nikitin, and M. Quack, Chem. Phys. **356**, 131 (2009).

[18] X. G. Wang and E. L. Sibert, J. Chem. Phys. **111**, 4510 (1999).

[19] P. Maroni, D. C. Papageorgopoulos, M. Sacchi, T. T. Dang, R. D. Beck, and T. R. Rizzo, Phys. Rev. Lett. **94**, 246104 (2005).

[20] L. Halonen, S. L. Bernasek, and D. J. Nesbitt, J. Chem. Phys. **115**, 5611 (2001).

[21] S. Nave and B. Jackson, Phys. Rev. B **81**, 233408 (2010).

[22] A. C. Luntz, J. Chem. Phys. **113**, 6901 (2000).

[23] L. B. F. Juurlink, D. R. Killelea, and A. L. Utz, Prog. Surf. Sci. **84**, 69 (2009).

[24] C. Díaz and R. A. Olsen, J. Chem. Phys. **130**, 094706 (2009).

[25] R. Milot and A. P. J. Jansen, Phys. Rev. B **61**, 15657 (2000).